Threshold model with anticonformity under random sequential updating

Bartłomiej Nowak [1,*] Michel Grabisch [2,†] and Katarzyna Sznajd-Weron [1,‡]

[1] *Department of Theoretical Physics, Faculty of Fundamental Problems of Technology, Wrocław University of Science and Technology, 50-370 Wrocław, Poland*

[2] *University of Paris I Panthéon-Sorbonne, Paris School of Economics, 106-112 Boulevard de l'Hôpital, 75013 Paris, France*

(Received 7 February 2022; accepted 15 May 2022; published 31 May 2022)

We study an asymmetric version of the threshold model of binary decision making with anticonformity under an asynchronous update mode that mimics continuous time. We analyze this model on a complete graph using three different approaches: the mean-field approximation, Monte Carlo simulation, and the Markov chain approach. The latter approach yields analytical results for arbitrarily small systems, in contrast to the mean-field approach, which is strictly correct only for an infinite system. We show that, for sufficiently large systems, all three approaches produce the same results, as expected. We consider two cases: (1) homogeneous, in which all agents have the same tolerance threshold, and (2) heterogeneous, in which thresholds are given by a beta distribution parametrized by two positive shape parameters α and β. The heterogeneous case can be treated as a generalized model that reduces to a homogeneous model in special cases. We show that particularly interesting behaviors, including social hysteresis and critical mass reported in innovation diffusion, arise only for values of α and β that yield the shape of the distribution observed in reality.

DOI: 10.1103/PhysRevE.105.054314

I. INTRODUCTION

Within the broad class of two-state dynamics [1], threshold models are particularly useful for describing various social and economic phenomena [2–4]. As in other binary-state opinion dynamics [5], the threshold model describes the social influence in decision making for the choice between precisely two alternatives, often denoted by 1 (agree, adopt, be active, etc.) and 0 (disagree, refuse, be inactive, etc.). Although a binary decision framework seems to be oversimplified, it is relevant for surprisingly many complex problems [3].

In the original threshold models of collective behavior proposed by Schelling [6] and Granovetter [2], an agent takes action 1 if the proportion of his neighbors in state 1 exceeds some threshold, otherwise action 0 is taken. It means that an agent in state 1 may return to state 0, because not enough neighbors are active. On the other hand, in many other threshold models, the transition from state 1 to state 0 is forbidden [3,7,8].

Here, we will use the original formulation, in which a transition from 1 to 0 is possible, as in [2,9,10], but additionally in the presence of anticonformity. Such a model has been already studied from a mathematical point of view under the synchronous update mode [10], considering a complete network or a random neighborhood. The study focused on finding absorbing classes, cycles, etc. In this paper, we investigate the same model but under random sequential updating (asynchronous updating), which mimics continuous time, and restricting to the complete network. Quick analysis shows that the two models behave very differently. Under the complete network assumption, the synchronous updating is a deterministic model and causes the appearance of cycling phenomena, in a way which is very dependent on the parameters chosen. In contrast, asynchronous updating is probabilistic and prevents the appearance of cycles. We show that it behaves similarly to a random-walk process. The appropriate tools in this situation are the phase transitions and phase diagrams under the mean-field approximation, which are typical for statistical physics of opinion formation [11–15], and also the Markov chain approach. It should be noted that phase transition diagrams cannot be used in the case of cycling, as only steady states can be studied.

We study the model on a complete graph since in this case the mean-field method allows us to obtain rigorous results. Independently, we conducted Monte Carlo simulations to validate the theoretical approach. Finally, we present a Markov chain approach, which allows us not only to obtain results for arbitrary small systems but also to derive the stationary distribution of visited states.

II. MODEL

We consider a society of n agents placed at the vertices of an arbitrary graph $G = (N, E)$, where $N = \{1, \ldots, n\}$ is a set of vertices (agents) and E is the set of undirected edges. Each agent i has a set of neighbors $K_i = \{j \in N : \{i, j\} \in E\}$, and the cardinality of this set $|K_i| = k_i$ is the degree of agent i. Here we assume that each agent belongs to its own neighborhood to avoid the unrealistic effect that the agent does not consider its own state at all. However, this assumption is only relevant when the neighborhood is small, which is

*bartlomiej.nowak@pwr.edu.pl
†michel.grabisch@univ-paris1.fr
‡katarzyna.weron@pwr.edu.pl

obviously not the case for an infinite complete graph. As in many other models, an agent can be in one of two alternative states: 1 (agree, adopt, be active, etc.) or 0 (disagree, refuse, be inactive, etc.). Following [10], we use the term "active" for agents in state 1, and "inactive" for agents in state 0, and denote by $a_i(t)$ the state (action) taken by agent i at time t.

We consider two types of social response, anticonformity and conformity, which occur with complementary probabilities p and $1-p$ respectively. In both cases, an agent can change its state if the ratio of active neighbors is above its tolerance threshold $r_i \in [0, 1]$. The threshold r_i of each agent is the realization of the random variable R with arbitrary distribution function $F_R(r)$ and does not change over time. In case of conformity, an agent follows the others, whereas in case of anticonformity he takes an opposite state to others. Therefore, the dynamics of the agent's state in the case of conformity can be written as [10]

$$a_i(t+\Delta t) = \begin{cases} 1 & \text{if } \frac{1}{k_i}\sum_{j\in K_i} a_j(t) \geqslant r_i, \\ 0 & \text{otherwise,} \end{cases} \tag{1}$$

whereas in case of anticonformity [10]

$$a_i(t+\Delta t) = \begin{cases} 0 & \text{if } \frac{1}{k_i}\sum_{j\in K_i} a_j(t) \geqslant r_i, \\ 1 & \text{otherwise.} \end{cases} \tag{2}$$

In this paper, we use the random sequential update mode, which means that an elementary update consists of

(1) random drawing of agent i from all n agents;

(2) with probability p agent i anticonforms to the neighborhood, that is, takes action $a_i(t+\Delta t)$ according to Eq. (2);

(3) with complementary probability $1-p$ agent i conforms to the neighborhood, that is, takes action $a_i(t+\Delta t)$ according to Eq. (1);

(4) time is updated: $t := t + \Delta t$.

As usual, $\Delta t = 1/n$ which means that the time unit consists of n elementary updates, which corresponds to one Monte Carlo step (MCS).

III. TRANSITION PROBABILITIES

Since we limit our study to the complete graph, we can fully describe the state of the system using a single random variable:

$$c = \frac{n_1}{n}, \tag{3}$$

where n_1 is the number of agents in the state 1 and thus c is the ratio of active agents. Therefore, there are $n+1$ possible states of the system: $0, \frac{1}{n}, \frac{2}{n}, \ldots, 1$.

Because we use the sequential (asynchronous) update mode, at most one agent can change its state at a time, and thus we can introduce the following transition probabilities:

$$\gamma^+(c) = \Pr\left(c(t+\Delta t) = c(t) + \frac{1}{n}\right),$$
$$\gamma^-(c) = \Pr\left(c(t+\Delta t) = c(t) - \frac{1}{n}\right). \tag{4}$$

For our model, the explicit form of these probabilities can be written, according to the algorithm described in the previous section, as follows:

$$\gamma^+(c) = (1-p)(1-c)\Pr(R \leqslant c) + p(1-c)\Pr(R > c),$$
$$\gamma^-(c) = (1-p)c\Pr(R > c) + pc\Pr(R \leqslant c), \tag{5}$$

where $\Pr(R \leqslant c)$ is the probability that the concentration c of the active agents is greater than or equal to the threshold R of the considered agent. This probability is simply the value of the cumulative distribution function $F_R(r)$ at $r = c$. Similarly, $\Pr(R > c)$ is the probability that the concentration of active voters does not exceed the threshold of considered agents, and thus it is equal to $1 - F_R(c)$. Therefore, we obtain

$$\gamma^+(c) = (1-p)(1-c)F_R(c) + p(1-c)[1-F_R(c)],$$
$$\gamma^-(c) = (1-p)c[1-F_R(c)] + pcF_R(c). \tag{6}$$

As can be seen from Eq. (4), the concentration of active agents c is a random variable. However, we can easily write the evolution equation for the expected value of c. Moreover, for $n \to \infty$ we can assume that c is localized to the expectation value. Therefore, we can write [5]

$$\frac{dc}{dt} = \gamma^+(c) - \gamma^-(c) \equiv f(c), \tag{7}$$

where $f(c)$ can be interpreted as an effective force acting on the system. Such a force will later allow us to introduce a potential that helps visualize the dynamics of the system [16]. As usual, we focus on the steady states, i.e., those for which

$$\frac{dc}{dt} = 0. \tag{8}$$

In the next two sections, we will use condition (8) to calculate the stationary concentration of active agents for two cases: (1) homogeneous, in which all agents have the same tolerance threshold, and (2) heterogeneous, in which the distribution of thresholds $F_R(r)$ is given by the beta distribution. We will compare the analytical results with the results of Monte Carlo simulations for the system of size $n = 10^4$, averaged over ten independent runs collected after 10^4 Monte Carlo steps. For the Monte Carlo simulations, two types of initial conditions will be used to reproduce all stable solutions of Eq. (8): (1) all agents initially active, which will be denoted by $c(0) = 1$, and (2) all agents initially inactive, which will be denoted by $c(0) = 0$.

IV. ONE THRESHOLD

In this case, the random variable R takes one value for all agents in the system, that is, all voters have the same threshold r:

$$F_R(c) = \mathbf{1}_{\{r\leqslant c\}},$$
$$1 - F_R(c) = \mathbf{1}_{\{r>c\}}, \tag{9}$$

where $\mathbf{1}_{\{r\leqslant c\}} = 1$ when $r \leqslant c$ and 0 otherwise. Inserting (9) into Eq. (6) and then into Eq. (7) we obtain

$$\frac{dc}{dt} = (1-p)[(1-c)\mathbf{1}_{\{r\leqslant c\}} - c\mathbf{1}_{\{r>c\}}] + p[(1-c)\mathbf{1}_{\{r>c\}} - c\mathbf{1}_{\{r\leqslant c\}}]. \tag{10}$$

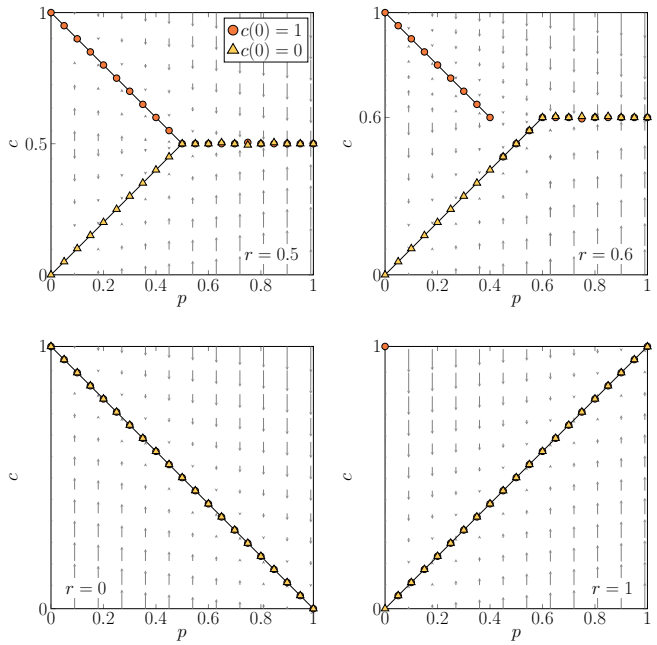

FIG. 1. Dependency between the stationary concentration of active agents c and the probability of anticonformity p for the model with one threshold for different values of the parameter r (indicated in the plots). Solid lines represent stable fixed points obtained analytically from Eq. (16). Symbols represent Monte Carlo simulations from two initial conditions indicated in the legend. Arrows indicate the flow in the system. The length of each arrow corresponds to the value of velocity $\frac{dc}{dt}$ given by Eq. (10).

From (10), we obtain several trivial fixed points:

$$(p = 0,\ c = 0) \qquad \forall r \neq 0, \tag{11}$$

$$(p = 1,\ c = 0) \qquad r = 0, \tag{12}$$

$$(p = 0,\ c = 1) \qquad \forall r \in [0, 1], \tag{13}$$

$$(p = 0.5,\ c = 0.5) \qquad \forall r \in [0, 1], \tag{14}$$

$$(p = 1 - r,\ c = r) \qquad \forall r \in [0, 1]. \tag{15}$$

The remaining solutions can be obtained by solving Eq. (8), which leads to

$$p = \frac{\mathbf{1}_{\{r \leqslant c\}} - c}{\mathbf{1}_{\{r \leqslant c\}} - \mathbf{1}_{\{r > c\}}}, \tag{16}$$

which is equivalent to the following cases:

$$\forall c < r \ \ p = c, \quad \forall c \geqslant r \ \ p = 1 - c. \tag{17}$$

From the above analysis, we do not obtain the steady state for any value of $r \in [0, 1]$ if $p \geqslant r$ for $r > 0.5$ or $p > 1 - r$ for $r \leqslant 0.5$. However, from the evolution of Eq. (10), represented by solid lines in Fig. 1, and from Monte Carlo simulations, represented by symbols in Fig. 1, we see that the system approaches the state $c = r$ for $p > r$. This raises the question of what the evolution of the system actually looks like. To answer this question we can provide at least three alternative approaches. We decided to present all three because we believe that there is value in showing the different possibilities of system analysis, especially given the interdisciplinary nature of the work. The composition of the authors themselves is also interdisciplinary, and each of us found a different method more compelling/intuitive.

The first, which is the most basic technique used to analyze dynamical systems, consists of interpreting a differential equation as a vector field [16]. Within this graphical way of thinking, we draw the arrows representing the flow dc/dt in the plane of model parameters, as shown in Fig. 1. The second method is based directly on the transition probabilities $\gamma^+(c), \gamma^-(c)$. If we split the transition probabilities into cases,

$$\begin{aligned} &\forall c < r \ \ \gamma^+(c) = p(1 - c) \ \wedge \ \gamma^-(c) = (1 - p)c, \\ &\forall c \geqslant r \ \ \gamma^+(c) = (1 - p)(1 - c) \ \wedge \ \gamma^-(c) = pc. \end{aligned} \tag{18}$$

we easily observe that they do not cross at any point, when $\forall r > 0.5 \ \ p \geqslant r$ or $\forall r \leqslant 0.5 \ \ p > 1 - r$; see the fourth column of Fig. 2. This implies no steady state. On the other hand, for $p < r$ transition probabilities $\gamma^-(c)$ and $\gamma^+(c)$ cross each other, as shown in the first three columns of Fig. 2, i.e., the steady state $\gamma^-(c) = \gamma^+(c)$ exists.

The third method is based on the idea of potential $V(c)$ [16]:

$$V(c) = -\int f(c)dc. \tag{19}$$

From Eq. (18) we see that the effective force $f(c)$ defined in Eq. (7) takes the following form:

$$f(c) = \gamma^+(c) - \gamma^-(c) = \begin{cases} p - c & \text{for } c < r, \\ 1 - p - c & \text{for } c \geqslant r, \end{cases} \tag{20}$$

and thus

$$V(c) = \begin{cases} -\int (p - c)dc = \frac{c^2}{2} - cp & \text{for } c < r, \\ -\int (1 - p - c)dc = \frac{c^2}{2} - c(1 - p) & \text{for } c \geqslant r. \end{cases} \tag{21}$$

Using such an approach, we draw a ball sliding down the walls of a potential well [16], as shown in Fig. 2. It should be noted that potentials given by Eq. (21) are determined up to a constant. Therefore, the size of the jump at the border $c = r$ is not unambiguously defined. Here, we have assumed that both constants are equal to zero, but this does not influence the dynamics of the system since the system cannot jump from one to the other potential minima, as presented in Fig. 2. This is because the point $c = r$ belongs only to one area and thus the dynamics from this point is uniquely defined no matter what jump is at $c = r$.

The steady states are the local extrema of $V(c)$. From Eq. (21) we see that the potential has a discontinuity at $c = r$, which implies no maximum (unstable steady state). Still,

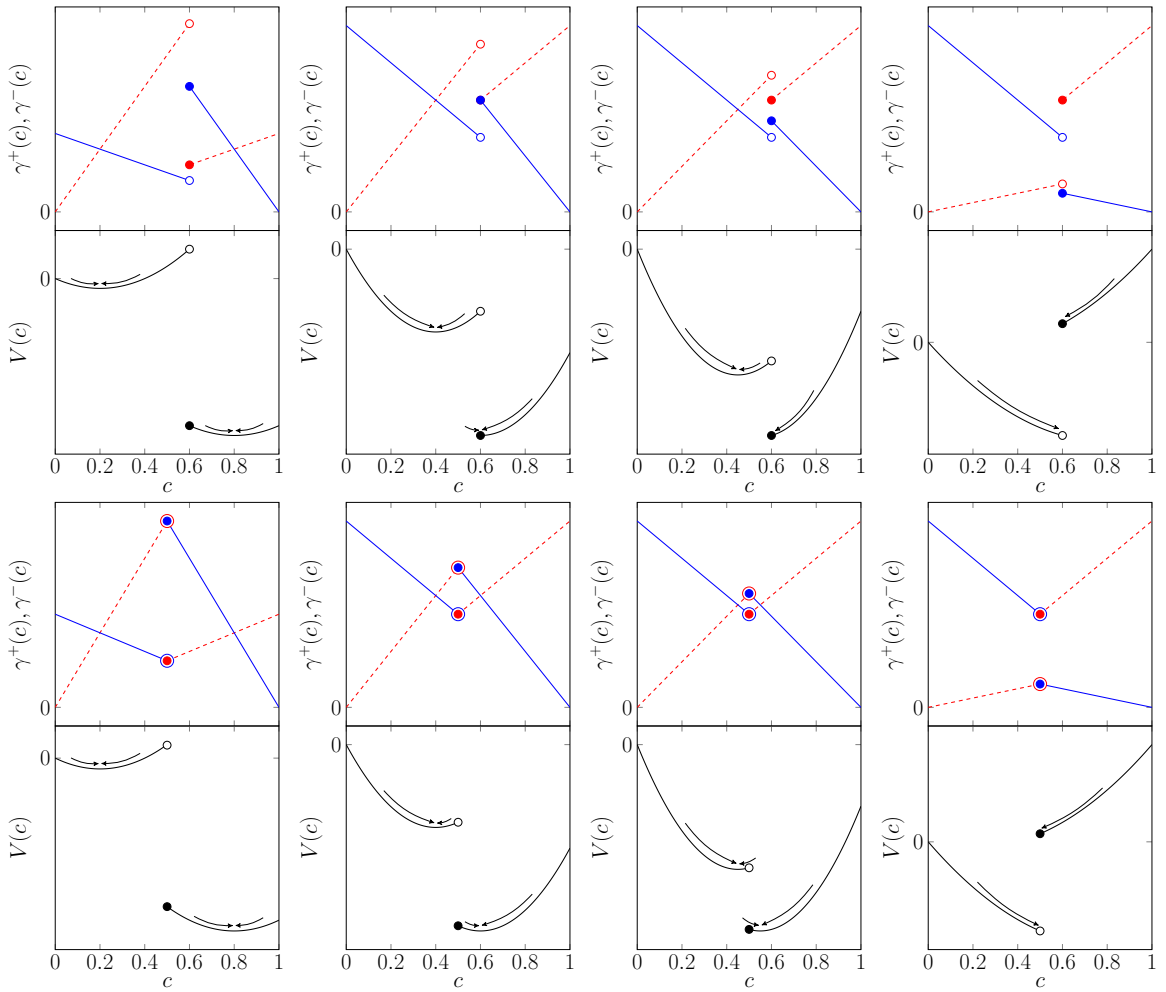

FIG. 2. Analysis of the steady states and the stability of the system for two values of threshold $r = 0.6$ (two first rows) and $r = 0.5$ (two last rows) and four values of $p = 0.2$ (first column), $p = 0.4$ (second column), $p = 0.45$ (third column), $p = 0.8$ (fourth column). In first and third rows, solid lines represents values of γ^+ and dotted lines stands for γ^- obtained with Eq. (18). Potentials $V(c)$ (second and fourth rows) are obtained with Eq. (21). In all subplots, filled circles denote continuity, while empty circles denote lack of continuity at this point.

at most two minima (stable steady states) are possible. In general, the number of minima, denoted by $M(r, p)$, can be described as follows:

$$\forall r > 0.5 \;\; M(r,p) = \begin{cases} 2 & \text{for } p \leqslant 1-r, \\ 1 & \text{for } 1-r < p < r, \\ 0 & \text{for } p \geqslant r, \end{cases} \tag{22}$$

$$\forall r \leqslant 0.5 \;\; M(r,p) = \begin{cases} 2 & \text{for } p < r, \\ 1 & \text{for } r \leqslant p \leqslant 1-r, \\ 0 & \text{for } p > 1-r. \end{cases} \tag{23}$$

In conclusion, despite the lack of steady state in the case $M(r, p) = 0$ we can observe that the flow of the system is towards the point $c = r$. It reaches an asymptotic minimum at this point because from both the left and right boundaries, the system flow is towards this minimum. This explains the behavior shown in Fig. 1, which was at first incomprehensible and inspired the above analysis.

V. BETA DISTRIBUTION

In the previous section, we studied the homogeneous system, in which all agents had the same value of the tolerance threshold r. However, we can also consider more general distributions of thresholds, allowing for heterogeneity. The most useful are distributions whose support values $r \in [0, 1]$ and show a variety of shapes. This is the case of the beta distribution with two parameters α and β, previously considered, for the models of tolerance without anticonformity [4]. It has a well-defined cumulative distribution function:

$$F_R(r) = I_r(\alpha, \beta) = \frac{B(r, \alpha, \beta)}{B(\alpha, \beta)}, \tag{24}$$

where $I_r(\alpha, \beta)$ is the regularized incomplete beta function, which can be defined in terms of the incomplete beta function $B(r, \alpha, \beta)$ and the complete beta function $B(\alpha, \beta)$. Inserting $F_R(r)$ given by Eq. (24) into (6) we obtain the transition probabilities $\gamma^+(c), \gamma^-(c)$. Then inserting them to Eq. (7) we get

$$\frac{dc}{dt} = (1-p)[(1-c)I_c(\alpha,\beta) - c(1-I_c(\alpha,\beta))] + p[(1-c)(1-I_c(\alpha,\beta)) - cI_c(\alpha,\beta)]. \tag{25}$$

Again, we can point out the obvious steady states ($p = 0,\ c = 0$), ($p = 0,\ c = 1$) for arbitrary values of α and β. For

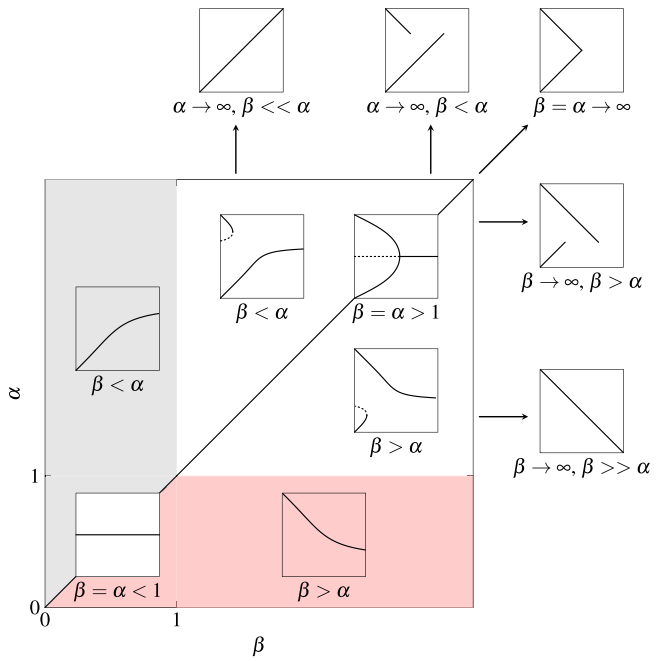

FIG. 3. Phase diagram for the heterogeneous model with thresholds described by the beta distribution parametrized by two shape parameters α and β. Each inset shows representative behavior of $c(p)$ for a given area of the phase diagram. Solid lines in the insets correspond to stable stationary states, whereas dashed lines correspond to unstable stationary states.

$c = 1/2$ formula (25) boils down to

$$\left.\frac{dc}{dt}\right|_{c=\frac{1}{2}} = \left(I_{\frac{1}{2}}(\alpha,\beta) - \frac{1}{2}\right)(1-2p), \tag{26}$$

which has two roots. The first one $p = 1/2$ gives the fixed point ($p = \frac{1}{2}, c = \frac{1}{2}$). The other root $I_{\frac{1}{2}}(\alpha,\beta) = \frac{1}{2}$ exists if the beta distribution is symmetric around the value $\frac{1}{2}$. This happens for $\alpha = \beta$, which leads to the conclusion that the value $c = \frac{1}{2}$ is a fixed point for all values of p if $\alpha = \beta$. For all remaining solutions we have the following relation:

$$p = \frac{I_c(\alpha,\beta) - c}{2I_c(\alpha,\beta) - 1}. \tag{27}$$

The information about the stability of the steady state is given by the sign of the derivative

$$\frac{dF}{dc} = \frac{c^{\alpha-1}(1-c)^{\beta-1}\Gamma(\alpha+\beta)}{\Gamma(\alpha)\Gamma(\beta)}(1-2p) - 1. \tag{28}$$

The state is stable if the above derivative is negative and unstable otherwise. The overall behavior of the model is summarized in Fig. 3. In the insets of this figure the dependence between the stationary value of c and parameter p is shown. Two shaded areas in Fig. 3 correspond to the situation in which at least one of the parameters α, β is smaller than 1. In this case, for $p > 0$ there is always only one steady state and c is monotonically increasing ($\beta < \alpha$), monotonically decreasing ($\beta > \alpha$), or constant ($\beta = \alpha$) function of p.

Recalling the shape of the probability density function (PDF) of the beta distribution, we can draw some conclusions. If the PDF of the tolerance threshold is a monotonically decreasing function of the threshold r, then the concentration of active agents decreases with the probability of anticonformity p, and vice versa. If the PDF has the highest values at $r = 0$ and $r = 1$, being a convex function of r, then for all values of $p > 0$ the stationary value of active agents is 0.5.

The most complex behavior is seen if both shape parameters α, β are greater than 1 but not infinitely large, which corresponds to a unimodal PDF, with zero probabilities at both end of the interval range, i.e., at $r = 0$ and $r = 1$. This case correspond to moderate tolerance [4], and it is a typical shape of the distribution of actual trait manifestations in behavior, as reported by psychologists [17]. In such a case, the phase transitions appear, as shown in Fig. 3. As long as $\beta = \alpha$, which corresponds to the symmetric PDF, there is a continuous phase transition between the phase in which one type of agent (active or inactive) dominates, and the symmetrical phase without the domination. The critical point, at which this transition occurs, can be calculated by solving the equation

$$\left.\frac{dF}{dc}\right|_{c=\frac{1}{2}} = 0, \tag{29}$$

which gives

$$p_1^* = \frac{1}{2} - \frac{\Gamma^2(\alpha)}{2^{3-2\alpha}\Gamma(2\alpha)}. \tag{30}$$

For $\alpha \neq \beta$, as long as shape parameters are finite and at least one of them is larger than 1, we obtain an interesting behavior, with the jump at some value of $p = p^*$ and hysteresis, as shown in Fig. 3. This can be especially useful to describe the innovation diffusion. For example, if $\beta > \alpha$ then for the small value of $p < p^*$ there is possibility of high adoption if the initial fraction of adopted is above the critical mass. However, if the initial fraction of adopted is too low, i.e., below the critical mass, the innovation cannot spread in the society. Similar behavior has been recently reported for the completely different mathematical model of the collective decision making with social learners for unequal merit options [18].

It is worth noticing that for $\alpha, \beta \to \infty$ we can recover the solution for the model with one threshold, as shown in Fig. 3. We are able to do that by recalling the formula giving the mode of the beta distribution with $\alpha, \beta > 1$:

$$m = \frac{\alpha - 1}{\alpha + \beta - 2}. \tag{31}$$

While $\alpha, \beta \to \infty$, the beta distribution is a one-point degenerate distribution with probability 1 at the midpoint m and 0 elsewhere. Thus, to obtain the case with the mode at the point $m = r$, i.e., recover the distribution for one threshold, parameters α and β should follow the formula

$$\beta = \frac{(1-r)\alpha - 1 + 2r}{r} \tag{32}$$

for $\alpha, \beta \to \infty$.

All results obtained analytically for beta distribution can be also obtained by Monte Carlo simulations, as shown in Fig. 4.

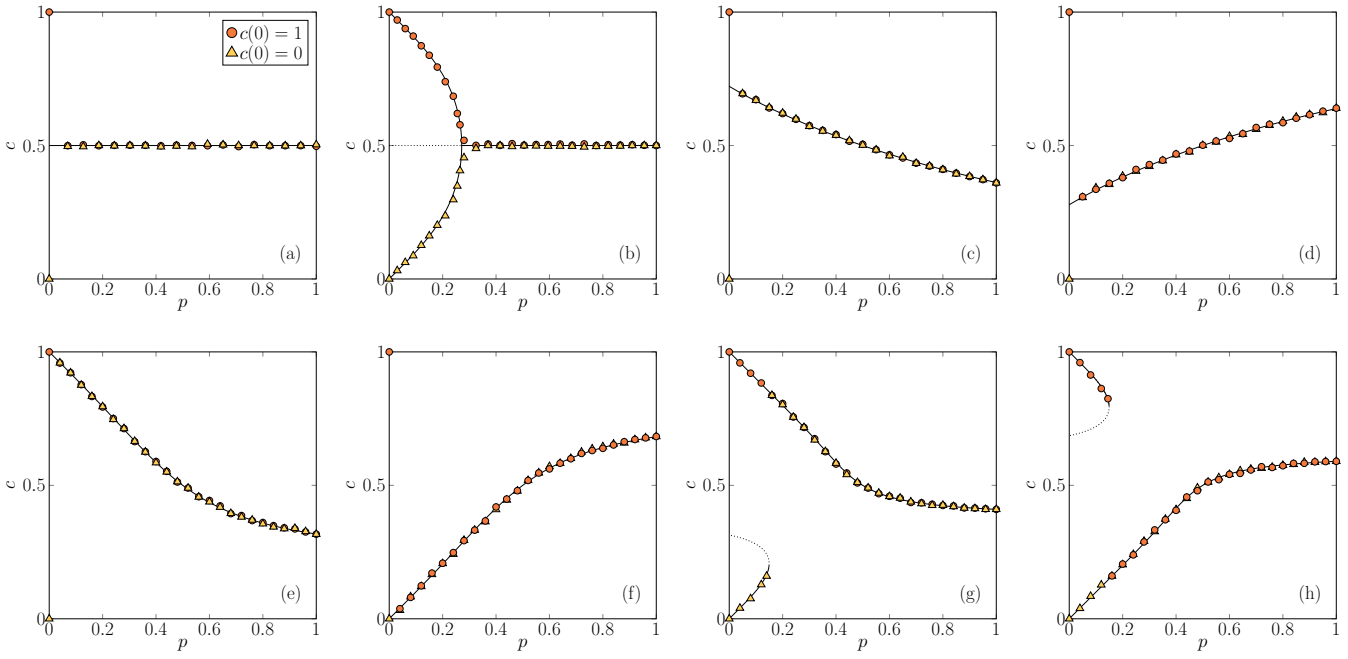

FIG. 4. Representative dependencies between the stationary concentration of spins up and the probability of anticonformity for model with beta distribution for different values of the parameters α and β: (a) $\alpha = \beta \leqslant 1$, (b) $\alpha = \beta > 1$, (c) $\alpha < \beta < 1$; α close to β, (d) $1 > \alpha > \beta$; α close to β, (e) $\alpha \leqslant 1 \ \wedge \ \alpha < \beta$, (f) $\beta \leqslant 1 \ \wedge \ \alpha > \beta$, (g) $1 < \alpha < \beta$, (h) $\alpha > \beta > 1$. Solid and dotted lines represent stable and unstable steady states respectively, obtained with Eq. (27). The exact values of parameters in the plots are as follows: (a) $\alpha = \beta = 0.9$; (b) $\alpha = \beta = 4$; (c) $\alpha = 0.1$, $\beta = 0.2$; (d) $\alpha = 0.2$, $\beta = 0.1$; (e) $\alpha = 1$, $\beta = 3$; (f) $\alpha = 3$, $\beta = 1$; (g) $\alpha = 5$, $\beta = 8$; (h) $\alpha = 8$, $\beta = 5$. Symbols represent Monte Carlo simulations from two initial conditions, denoted in the legend. The results are averaged over ten runs and collected after 10^4 MCS for system of size 10^4.

VI. MARKOV CHAIN APPROACH

Previously, we were assuming that the size of the system is infinite, i.e., $n \to \infty$. However, such an assumption is not very realistic for social systems. Actually, social scientists are often interested in small systems. Therefore, in this section, we make analysis of the convergence of c in the long run using Markov chains for arbitrary small systems. The advantage of the Markov chain approach in the context of agent-based modeling of opinion dynamics has been already reported in [19].

Transition probabilities given by Eq. (4) allows us to write the $(n+1) \times (n+1)$ transition matrix, whose general term (i, j) indicates the probability of transition from state i to state j. Due to the asynchronous update mode, $\mathbf{P}$ is a tridiagonal row-stochastic matrix:

$$\mathbf{P} = \begin{bmatrix} \gamma^0(0) & \gamma^+(0) & 0 & 0 & \cdots & 0 \\ \gamma^-\left(\frac{1}{n}\right) & \gamma^0\left(\frac{1}{n}\right) & \gamma^+\left(\frac{1}{n}\right) & 0 & \cdots & 0 \\ 0 & \gamma^-\left(\frac{2}{n}\right) & \gamma^0\left(\frac{2}{n}\right) & \gamma^+\left(\frac{2}{n}\right) & \cdots & 0 \\ 0 & \cdots & \ddots & \ddots & \ddots & 0 \\ 0 & \cdots & 0 & \gamma^-\left(\frac{n-1}{n}\right) & \gamma^0\left(\frac{n-1}{n}\right) & \gamma^+\left(\frac{n-1}{n}\right) \\ 0 & \cdots & 0 & 0 & \gamma^-(1) & \gamma^0(1) \end{bmatrix} \tag{33}$$

with $\gamma^0(c) = 1 - \gamma^+(c) - \gamma^-(c)$. This process is a random walk process. Its transition graph is strongly connected and aperiodic, hence $\mathbf{P}$ is a primitive matrix, i.e., the only absorbing class is the set of all states. This means that in the long run, the system at time t can be in any of the $n+1$ states, and there is no stabilization [20,21].

From Markov chain theory, the limit vector $\pi = [\pi(0), \ldots, \pi(c), \ldots, \pi(1)]^T$ giving the probability $\pi(c)$ to be in state c in the long run is obtained as the left normalized eigenvector of $\mathbf{P}$ associated with eigenvalue 1, i.e., π is the solution of the linear system in variable z

$$(\mathbf{P}^T - I)z = 0, \quad \mathbf{1}^T z = 1 \tag{34}$$

with $\mathbf{1} = (1, \ldots, 1)^T$. From now on, to avoid heavy notation, we denote $\gamma^+(k/n)$ by $\gamma^+(k)$, and similarly for $\gamma^-(k/n)$,

$\pi(k/n)$, etc. We obtain

$$\mathbf{P}^T - I = \begin{bmatrix} -\gamma^+(0) & \gamma^-(1) & 0 & 0 & 0 & \cdots & 0 \\ \gamma^+(0) & -\gamma^-(1)-\gamma^+(1) & \gamma^-(2) & 0 & 0 & \cdots & 0 \\ 0 & \ddots & \ddots & \ddots & 0 & \cdots & 0 \\ 0 & \cdots & \gamma^+(k-1) & -\gamma^-(k)-\gamma^+(k) & \gamma^-(k+1) & \cdots & 0 \\ 0 & \cdots & 0 & \ddots & \ddots & \ddots & 0 \\ 0 & \cdots & 0 & 0 & \gamma^+(n-2) & -\gamma^-(n-1)-\gamma^+(n-1) & \gamma^-(n) \\ 0 & \cdots & 0 & 0 & 0 & \gamma^+(n-1) & -\gamma^-(n) \end{bmatrix}. \tag{35}$$

Solving the system yields

$$\begin{aligned} \pi(0) &= \frac{\gamma^-(1)}{\gamma^+(0)}\pi(1), \\ \pi(1) &= \frac{\gamma^-(2)}{\gamma^+(1)}\pi(2), \\ &\vdots = \vdots \\ \pi(k) &= \frac{\gamma^-(k+1)}{\gamma^+(k)}\pi(k+1), \\ &\vdots = \vdots \\ \pi(n-1) &= \frac{\gamma^-(n)}{\gamma^+(n-1)}\pi(n). \end{aligned} \tag{36}$$

This yields

$$\pi(k) = \frac{\gamma^+(k-1)}{\gamma^-(k)}\frac{\gamma^+(k-2)}{\gamma^-(k-1)}\cdots\frac{\gamma^+(0)}{\gamma^-(1)}\pi(0) \quad (k=1,\ldots,n). \tag{37}$$

In the case of one threshold we are able to derive the above formulas analytically. Using Eq. (18) we obtain

$$\begin{aligned} \pi(k) &= \frac{(1-p)(k+1)}{p(n-k)}\pi(k+1) && (k < rn-1), \\ \pi(k) &= \frac{k+1}{n-k}\pi(k+1) && (rn-1 \leqslant k < rn), \\ \pi(k) &= \frac{p(k+1)}{(1-p)(n-k)}\pi(k+1) && (k \geqslant rn). \end{aligned}$$

Let us find when $\pi(k)$ is increasing or decreasing. Supposing $k < rn-1$, we have

$$\begin{aligned} \frac{(1-p)(k+1)}{p(n-k)} \leqslant 1 &\Leftrightarrow (1-p)(k+1) \leqslant p(n-k) \\ &\Leftrightarrow k \leqslant p(n+1)-1. \end{aligned}$$

When $k \geqslant rn$, we obtain

$$\frac{p(k+1)}{(1-p)(n-k)} \leqslant 1 \Leftrightarrow k \leqslant n - p(n+1).$$

Therefore,

(1) For states below r, the peak is attained at

$$\hat{c}_1 = \frac{\hat{k}_1}{n}, \text{ with } \hat{k}_1 = \lceil p(n+1) \rceil - 1.$$

Observe that when n is large, this yields $\hat{c}_1 \approx p$.

(2) For states above r, the peak is attained at

$$\hat{c}_2 = \frac{\hat{k}_2}{n}, \text{ with } \hat{k}_2 = n - \lfloor p(n+1) \rfloor.$$

When n is large, we obtain $\hat{c}_2 \approx 1-p$.

Depending on the relative positions of p and r, there can be one or two peaks, as summarized as follows:

If $r \leqslant p$, $r \leqslant 1-p$: peak at $\hat{c}_2$,
if $p \leqslant r \leqslant 1-p$: two peaks at $\hat{c}_1, \hat{c}_2$,
if $1-p \leqslant r \leqslant p$: peak at $\frac{\lceil rn \rceil}{n}$,
$p \leqslant r$, $1-p \leqslant r$: peak at $\hat{c}_1$.

In the case where there are two peaks, i.e., $p \leqslant r \leqslant 1-p$, let us find the relative heights of the peaks. From (37), we find, assuming $rn \notin \mathbb{N}$,

$$\begin{aligned} \pi(\lfloor rn \rfloor) &= \pi(\hat{k}_1)\left(\frac{p}{1-p}\right)^{\lfloor rn \rfloor - \lceil p(n+1) \rceil + 1} \\ &\quad \times \frac{(n-\lfloor rn \rfloor + 1)\cdots(n-\lceil p(n+1) \rceil + 1)}{\lfloor rn \rfloor \cdots \lceil p(n+1) \rceil}, \\ \pi(\lfloor rn \rfloor + 1) &= \pi(\hat{k}_2)\left(\frac{p}{1-p}\right)^{n-\lfloor p(n+1) \rfloor - \lfloor rn \rfloor - 1} \\ &\quad \times \frac{(\lfloor rn \rfloor + 2)\cdots(n-\lfloor p(n+1) \rfloor)}{(n-\lfloor rn \rfloor - 1)\cdots(\lfloor p(n+1) \rfloor + 1)}, \\ \pi(\lfloor rn \rfloor + 1) &= \pi(\lfloor rn \rfloor)\frac{n-\lfloor rn \rfloor}{\lfloor rn \rfloor + 1}. \end{aligned}$$

Hence, assuming $p(n+1) \notin \mathbb{N}$,

$$\frac{\pi(\hat{k}_2)}{\pi(\hat{k}_1)} = \left(\frac{p}{1-p}\right)^{2\lfloor rn \rfloor - n + 1}. \tag{38}$$

When n is large, we obtain

$$\frac{\pi(\hat{k}_2)}{\pi(\hat{k}_1)} \approx \left(\frac{p}{1-p}\right)^{n(2r-1)+1}. \tag{39}$$

Observe that the peaks have equal heights when $p = 0.5$, and when $r = 0.5$ the ratio is equal to $p/(1-p)$.

Besides, we have solved numerically by SCILAB the system of equations (34), which is possible for reasonable values of n, and obtained its solution $\pi(k)$, $k = 0, \ldots, n$. Table I shows the value of the ratio of the two peaks for various values of p, r as given by Eq. (38), compared to the output of SCILAB. Figure 5 shows the computed distribution π for $n = 100$ for the one-threshold case and also the case of the beta distribution, compared to the histograms obtained from Monte Carlo simulations.

TABLE I. Example of results for $n = 10$ for different values of p and r under the condition $p \leqslant r \leqslant 1 - p$. In the table are presented the theoretical ratio given by Eq. (38) (left column), as well as the values $\pi(\hat{k}_1)$ and $\pi(\hat{k}_2)$ computed numerically and the ratio between them (three rightmost columns).

p	r	$\pi(\hat{k}_2)/\pi(\hat{k}_1)$	$\pi(\hat{k}_1)$	$\pi(\hat{k}_2)$	Ratio
0.21	0.41	3.7619048	0.064177	0.241429	3.7619052
0.21	0.61	0.0187835	0.2966234	0.005572	0.0187834
0.25	0.5	0.3333333	0.218683	0.0728942	0.3333334

We comment on these results. The Markov approach permits to obtain the stationary probability distribution of the different states, for any value of n, without approximation. It is found that in the long run, even if any state has a nonzero probability to be reached, some states have a much higher probability than the others to appear. In the case of one threshold, we have analytically proved the presence of one or two peaks, and their positions when n is large perfectly coincides with what was predicted by the mean-field approach. It is complementary to the results given by the mean-field approach, since the Markov approach is able to give the probability of occurrence of each stationary state. On the other hand, the complexity of the system of linear equations (34) induced by the Markov chain makes this approach not always tractable (e.g., with the beta distribution). Nevertheless, we have shown that for reasonably large values of n (e.g., $n = 100$), this linear system can be solved numerically, giving a perfect fit with theoretical values, as shown by Table I and with Monte Carlo simulations as well, see Fig 5.

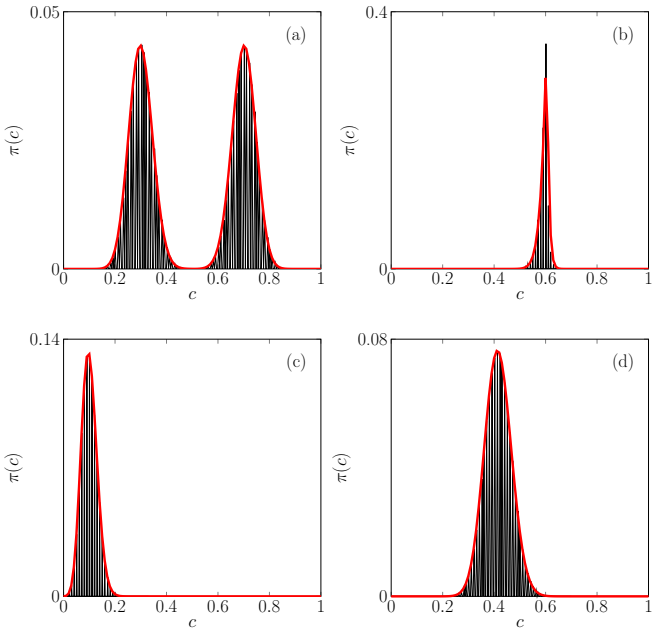

FIG. 5. Stationary distributions of visited states for model with one threshold (upper row) with parameters (a) $r = 0.5$, $p = 0.3$; (b) $r = 0.6$, $p = 0.7$ and model with beta distribution (bottom row) with parameters (c) $\alpha = 8$, $\beta = 5$, $p = 0.1$; (d) $\alpha = 3$, $\beta = 1$, $p = 0.4$. Solid red lines are distributions obtained with Markov approach, black histograms are obtained with trajectories from Monte Carlo simulations for system of size $n = 100$ and thermalization time $t = 2 \times 10^6$ MCS from 100 initial conditions evenly distributed on interval [0,1], averaged over 1000 independent runs.

VII. SUMMARY AND RESEARCH DIRECTIONS FOR THE FUTURE

In this paper, we investigated the threshold model with anticonformity under asynchronous update mode, which mimics continuous time. We considered two cases: (1) homogeneous, in which all agents had the same threshold, and (2) heterogeneous, in which the thresholds are given by the beta distribution function. The homogeneous case with $r = 0.5$ is identical to the homogeneous symmetrical threshold model with anticonformity [22]. Moreover, it is almost identical to the majority-vote process [23,24]. The only difference between the models is when the number of active and inactive agents in the neighborhood of a chosen agent is equal. In such a case, the state of the system does not change within the majority-vote model, whereas within the threshold model the change is possible. From this point of view, the threshold model with anticonformity under asynchronous updating can be treated as a generalization of a majority-vote model.

On the complete graph, the homogeneous threshold model does not give particularly interesting results. The relationship between the stationary ratio of active agents and the probability of anticonformity consists of linear dependencies, similarly to the homogeneous symmetrical threshold model [22,25]. The only interesting feature of this model is the discontinuity that appears at $c = r = 1 - p$ for $r > 0.5$ and at $c = r = p$ for $r < 0.5$. In the result, the system reaches one of two different steady states, depending on the initial conditions. Much richer behavior is observed in the heterogeneous model with thresholds given by the beta distribution function, parametrized by α, β, which allows tuning the model to the homogeneous one ($\alpha, \beta \to \infty$) and to the maximally heterogeneous one (i.e., described by the uniform distribution function).

A particularly interesting behavior is obtained if at least one of the shape parameters α or β is larger than 1 and both parameters are finite. In this case the PDF has a shape that resembles those of actual trait manifestation in behavior, as reported by psychologists [17], i.e., unimodal, not necessarily symmetrical, function with maximum at the value $0 < r < 1$. In such a case a phase transition appears, which is continuous for $\alpha = \beta$, and discontinuous otherwise. In the latter case, the transition involves phenomena typical of social systems, such as social hysteresis [26] and the critical mass [27–29].

The future research on the model can be conducted in several directions, related to the following questions:

(1) How would the results change if the threshold for anticonformity were different than that for conformity? This question is inspired by the work on the q-voter model with generalized anticonformity [30]. In the q-voter model such a generalization resulted in switching from continuous to discontinuous phase transitions for some values of parameters. The question is, are the same phenomena observed for the threshold model?

(2) How would the structure of a network influence the results? This question is inspired by the work on the symmetrical threshold [25]. It was shown that on random graphs with the degree observed empirically for social networks, the largest social hysteresis is observed for $r \in (0.65, 0.85)$. This was a meaningful result from the social point of view and thus it would be desirable to check if it appears also in the asymmetric model studied here.

(3) How would the results change if the quenched approach to anticonformity were used? In this version of the model, we used the annealed approach, in the sense that each agent could anticonform (with probability p) or conform (with probability $1 - p$). However, we could use also the quenched approach, in which a fraction p of agents are permanently anticonformists. This question is inspired by the work on the q-voter model with nonconformity under quenched and annealed approaches [31]. It was shown that on the complete graph both approaches give the same result for the q-voter model with anticonformity, but different results for the model with independence. The question is, to what extend is this result universal?

ACKNOWLEDGMENTS

This research was supported by the National Science Center (NCN, Poland) Grant No. 2019/35/B/HS6/02530.

[1] J. P. Gleeson, Binary-State Dynamics on Complex Networks: Pair Approximation and Beyond, Phys. Rev. X **3**, 021004 (2013).
[2] M. Granovetter, Threshold models of collective behavior, Am. J. Sociol. **83**, 1420 (1978).
[3] D. Watts, A simple model of global cascades on random networks, Proc. Natl. Acad. Sci. USA **99**, 5766 (2002).
[4] V. V. Breer, Models of tolerant threshold behavior (from T. Schelling to M. Granovetter), Autom. Remote Control **78**, 1304 (2017).
[5] A. Jędrzejewski and K. Sznajd-Weron, Statistical physics of opinion formation: Is it a SPOOF? C. R. Phys. **20**, 244 (2019).
[6] T. C. Schelling, *Micromotives and Macrobehavior* (Norton, New York, 1978).
[7] P. S. Dodds and D. J. Watts, Universal Behavior in a Generalized Model of Contagion, Phys. Rev. Lett. **92**, 218701 (2004).
[8] J. S. Juul and M. A. Porter, Hipsters on networks: How a minority group of individuals can lead to an antiestablishment majority, Phys. Rev. E **99**, 022313 (2019).
[9] E. Lee and P. Holme, Social contagion with degree-dependent thresholds, Phys. Rev. E **96**, 012315 (2017).
[10] M. Grabisch and F. Li, Anti-conformism in the threshold model of collective behavior, Dynamic Games and Applications **10**, 444 (2020).
[11] C. Castellano, S. Fortunato, and V. Loreto, Statistical physics of social dynamics, Rev. Mod. Phys. **81**, 591 (2009).
[12] S. Galam and A. Martins, Two-dimensional Ising transition through a technique from two-state opinion-dynamics models, Phys. Rev. E **91**, 012108 (2015).
[13] T. Raducha, M. Wilinski, T. Gubiec, and H. Stanley, Statistical mechanics of a coevolving spin system, Phys. Rev. E **98**, 030301(R) (2018).
[14] M. Calvelli, N. Crokidakis, and T. J. Penna, Phase transitions and universality in the Sznajd model with anticonformity, Physica A **513**, 518 (2019).
[15] A. R. Vieira, A. F. Peralta, R. Toral, M. S. Miguel, and C. Anteneodo, Pair approximation for the noisy threshold q-voter model, Phys. Rev. E **101**, 052131 (2020).
[16] S. H. Strogatz, *Nonlinear Dynamics and Chaos: With Applications to Physics, Biology, Chemistry, and Engineering*, 2nd ed. (CRC, Boca Raton, FL, 2015).
[17] W. Fleeson and P. Gallagher, The implications of Big Five standing for the distribution of trait manifestation in behavior: Fifteen experience-sampling studies and a meta-analysis, J. Pers. Soc. Psychol. **97**, 1097 (2009).
[18] V. Yang, M. Galesic, H. McGuinness, and A. Harutyunyan, Dynamical system model predicts when social learners impair collective performance, Proc. Nat. Acad. Sci. USA **118**, e2106292118 (2021).
[19] S. Banisch, R. Lima, and T. Araújo, Agent based models and opinion dynamics as markov chains, Soc. Netw. **34**, 549 (2012).
[20] J. G. Kemeny and J. L. Snell, *Finite Markov Chains* (Springer, Berlin, 1976).
[21] E. Seneta, *Non-negative Matrices and Markov Chains* (Springer, Belrin, 2006).
[22] B. Nowak and K. Sznajd-Weron, Homogeneous symmetrical threshold model with nonconformity: Independence versus anticonformity, Complexity **2019**, 14 (2019).
[23] T. M. Liggett, *Interacting Particle Systems* (Springer, Berlin, 1985).
[24] M. de Oliveira, Isotropic majority-vote model on a square lattice, J. Stat. Phys. **66**, 273 (1992).
[25] B. Nowak and K. Sznajd-Weron, Promoting discontinuous phase transitions by the quenched disorder within the multistate q-voter model, arXiv:2106.11238.
[26] M. Scheffer, F. Westley, and W. Brock, Slow response of societies to new problems: Causes and costs, Ecosystems **6**, 493 (2003).
[27] D. Centola, J. Becker, D. Brackbill, and A. Baronchelli, Experimental evidence for tipping points in social convention, Science **360**, 1116 (2018).
[28] C. Van Slyke, V. Ilie, H. Lou, and T. Stafford, Perceived critical mass and the adoption of a communication technology, Eur. J. Inf. Syst. **16**, 270 (2007).
[29] A. Mahler and E. M. Rogers, The diffusion of interactive communication innovations and the critical mass: The adoption of telecommunications services by German banks, Telecomm. Policy **23**, 719 (1999).
[30] A. Abramiuk-Szurlej, A. Lipiecki, J. Pawłowski, and K. Sznajd-Weron, Discontinuous phase transitions in the q-voter model with generalized anticonformity on random graphs, Sci. Rep. **11**, 17719 (2021).
[31] A. Jędrzejewski and K. Sznajd-Weron, Person-situation debate revisited: Phase transitions with quenched and annealed disorders, Entropy **19**, 415 (2017).